# Induced Circular Dichroism Spectra of α-, β- and γ-Cyclodextrin Complexes with Sodium 4'-Hydroxy-3'-isopropylazobenzene-4-sulfonate and Sodium 4'-Hydroxy-3',5'-diisopropylazobenzene-4-sulfonate

**Noboru Yoshida,*[a] Hiroyuki Yamaguchi[b] and Miwako Higashi[c]**
[a] *Laboratory of Molecular Functional Chemistry, Division of Material Science, Graduate School of Environmental Earth Science, Hokkaido University, Sapporo 060, Japan*
[b] *Faculty of Engineering, Department of Materials Science, Ibaraki University, Hitachi 316, Japan*
[c] *Center for Cooperative Research and Development, Ibaraki University, Hitachi 316, Japan*

The induced circular dichroism (ICD) spectra of α-, β- and γ-cyclodextrin complexes with sodium 4'-hydroxy-3'-isopropylazobenzene-4-sulfonate, 3-Pr$^i$(4-OH)$C_6H_3$–N=N–$C_6H_4SO_3^-Na^+$ **5** and sodium 4'-hydroxy-3',5'-diisopropylazobenzene-4-sulfonate, 3,5-(Pr$^i$)$_2$(4-OH)$C_6H_2$–N=N–$C_6H_4SO_3^-Na^+$ **8** in aqueous solution have been measured. ICD is observed on the absorption bands of the achiral azo guest molecules **5** and **8** which are included in the dissymmetric field of the chiral cyclodextrin (CD) cavity. The ICD spectral patterns change drastically depending on the shape and size of the alkyl substituents (R$^i$ and R$^j$) of the phenol moiety [R$^i$R$^j$(4-OH)$C_6H_2$–] of the azo guest molecules, R$^i$R$^j$(4-OH)$C_6H_2$–N=N–$C_6H_4SO_3^-Na^+$. The π→π* electronic transitions which are polarized along the long axis of the slim guest molecule **5** show almost a single positive ICD in all of the α-, β- and γ-CD inclusion complexes. This result indicates that the guest **5** is included from the long-axis side into the CD cavity. However, the ICD spectra of the β- and γ-CD complexes of the bulky guest molecule **8** show a split-type positive and negative ICD signal in the π→π* transition band. This splitting pattern may arise from the dimer formation of **8** in the form of the 2:2 (guest:CD) β- and γ-CD inclusion complexes.

The mechanism of the inclusion reactions between the alkyl-substituted azo molecules, $R^3R^5$(4-OH)$C_6H_2$–N=N–$C_6H_4$-$SO_3^-Na^+$ **1–8** and α-cyclodextrin (α-CD) has been elucidated from kinetic[1] and structural aspects.[2] Three types of reaction mechanisms depending on the shape and size of the alkyl substituents ($R^3$ and $R^5$) were found.

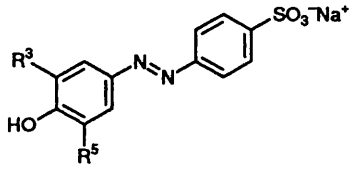


**1–8**

A one-step inclusion mechanism [eqn. (1)] was observed for

$$\alpha\text{-CD} + \text{Guest (G)} \rightleftharpoons \text{G–}\alpha\text{CD} \quad (1)$$

the guest systems **1** ($R^3 = R^5 = H$), **2** ($R^3$ = Me, $R^5 = H$) and **8** ($R^3 = R^5$ = Pr$^i$), whereas in the guest systems **4** ($R^3$ = Pr, $R^5 = H$), **5** ($R^3$ = Pr$^i$, $R^5 = H$) and **6** ($R^3$ = Bu$^s$, $R^5 = H$) a two-step inclusion mechanism [eqn. (2)] was found.[1] The guest

$$\alpha\text{-CD} + \text{Guest (G)} \rightleftharpoons \text{G–}\alpha\text{CD}^* \rightleftharpoons \text{G–}\alpha\text{CD} \quad (2)$$

molecules **3** ($R^3$ = Et, $R^5 = H$) and **7** ($R^3$ = Bu$^t$, $R^5 = H$) are borderline between the one- and two-step inclusion mechanism.

Although the structures of the final inclusion complexes (G–αCD) and the intermediate complexes (G–αCD*) are predicted from the analysis of $^1$H NMR spectra,[2] precise structural information, such as the orientation and the conformation of the guest molecule within the CD cavity, is not obtained. Furthermore, the structures of β-CD and γ-CD complexes of these guest systems have been little clarified so far.

Optical activity is induced in the achiral azo guests **1–8** in the presence of cyclodextrins. In general, induced circular dichroism (ICD) is expected on the absorption bands of the achiral guest molecules which interact with chiral host molecules such as cyclodextrin,[3] poly-α-amino acids,[4] proteins[5] and nucleic acids.[6] Multiple weak interacting forces such as van der Waals force, hydrogen bonding, hydrophobic interaction, electrostatic interaction, and/or charge-transfer force operate in synergy in all host–guest systems.

The shape and sign of ICD spectra of these systems provide precise structural information. Harata and Uedaira have measured the ICD spectra of β-CD complexes with naphthalene derivatives and estimated the orientation of the chromophore within the cavity of the β-CD.[7] If the direction of the electric dipole moment in the chromophore is parallel to the long axis of β-CD cavity, then the rotational strength gives a positive ICD value and the transition with the electric dipole moment perpendicular to the long axis gives a negative ICD value. This enables us to estimate the orientation of the chromophore within the cavity of β-CD if the direction of the electric dipole moment in the chromophore is known.[7] Recently, a further detailed study concerning the shape and sign of the ICD of the CD inclusion complexes has been extended by some authors.[8]

In the molecular stacking for natural anthocyanins[9] and synthetic cyanine dye[10] and in some host–guest systems[11] such as azo dye–CD, azo dye–polypeptides and azo dye–1-cyclohexyl-3-(2-morpholoethyl)carbodiimide metho-*p*-toluene-sulfonate, exciton split circular dichroism spectra have been observed if sufficiently strong electronic transitions exist. The result of exciton splitting of excited states in the molecular aggregates may be the appearance of a split ICD spectral pattern which results from spatial interactions such as stacking between two or more chromophores.

In this paper, the azo guest molecules **1–8** were used and ICD spectra of the inclusion complexes with α-, β- and γ-cyclodextrin were investigated. The ICD spectra of these

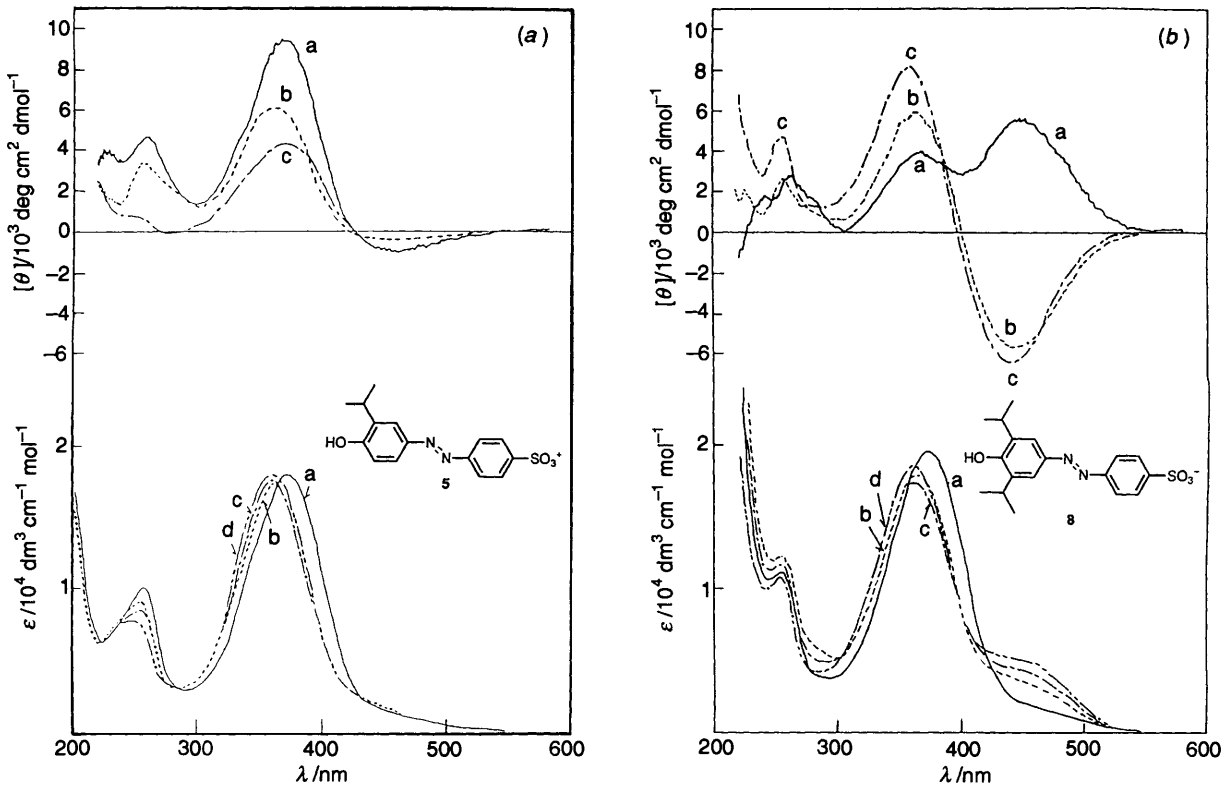


**Fig. 1** Induced circular dichroism (top) and absorption (bottom) spectra of the α-, β- and γ-cyclodextrin complexes of **5** (*a*) and **8** (*b*) at pH 4 and 25 °C. [**5**] = 4.53 × $10^{-5}$ mol $dm^{-3}$ and [**8**] = 4.51 × $10^{-5}$ mol $dm^{-3}$. (**a**) [α-CD] = 8 × $10^{-3}$ mol $dm^{-3}$; (**b**) [β-CD] = 8 × $10^{-3}$ mol $dm^{-3}$; (**c**) [γ-CD] = 8 × $10^{-3}$ mol $dm^{-3}$; (**d**) guest only.

inclusion complexes will give precise structural information, since the optical activity will be induced by the specific interaction geometry between the guest and the cyclodextrins.

## Experimental

*Materials.*—Azo guest molecules used were purified as described previously.[1] α- and β-Cyclodextrin were obtained from Tokyo Kasei Kogyo Co. and used without further purification. γ-Cyclodextrin was obtained from Nihon Shokuhin Kako Co. Doubly-distilled and deionized water was used as the solvent. All other chemicals were reagent grade.

*Measurements.*—The absorption spectra were obtained with a Hitachi U-3200 recording spectrophotometer. The CD spectra were measured using a JASCO J-600C circular dichrometer. The magnetic circular dichroism (MCD) spectra were recorded with a JASCO J-600C instrument equipped with a 1.32 T electromagnet. In order to obtain an adequate signal-to-noise ratio, we used a computer for multiple scanning and averaging. Each memory unit in the computer stored the CD signal for a spectral band of 0.1 nm. The time constant, step resolution, scan speed and path length of the cell were 1.0 s, 0.4 nm, 50 nm $min^{-1}$ and 10 mm, respectively. The wavelengths of the sharp bands were accurate to within ±0.1 nm for absorption and ±0.2 nm for CD. All measurements were made on deaerated samples at room temperature. $[\theta]_M$ is molar ellipticity in $10^{-1}$ deg $dm^2$ $mol^{-1}$ $G^{-1}$.

## Results and Discussion

*Absorption and Induced CD Spectra of the Cyclodextrin Inclusion Complexes of* **5** *and* **8**.—Due to the lack of a chiral centre, both **5** and **8** are not expected to exhibit optical activity alone in aqueous solution. However, upon interacting with CD which has a chiral cavity, **5** and **8** induce positive enhancement in the π→π* band within 300–400 nm which can be assigned to the long-axis-polarized transition (Fig. 1). The ICD spectra of **5**–βCD and **5**–γCD show quite interesting differences compared with those of **8**–βCD and **8**–γCD. The β- and γ-CD complexes of **5** induce single ICD spectra [Fig. 1(*a*)], but those of **8** induce the split-type spectra [Fig. 1(*b*)]. The difference in structure of **5** and **8** is only in the number of isopropyl substituents on the phenol moiety. Needless to say, owing to the larger steric hindrance of the 3′,5′-diisopropylphenol moiety of **8**, α-CD does not bind from the 3′,5′-diisopropylphenol side.[1] Although β- and γ-CD have a larger cavity than α-CD, it is difficult for them to interact with **8** from the 3′,5′-diisopropylphenol side. Further details of these ICD spectra showed that the α-, β- and γ-CD inclusion complexes with **5** showed a strong positive ICD band at 350–370 nm and a weak negative ICD band at 450 nm, respectively [Fig. 1(*a*)]. The electronic absorption bands at 350–370 nm and 450 nm were assigned to the π→π* and n→π* transitions of the azo –N=N– group, respectively, from the results calculated by the CNDO method (*vide infra*). In the α-CD system, the shift of the absorption maximum ($\lambda_{max}$) due to the π→π* transition is much larger than that in the β- and γ-CD systems.

The orientation of the guest molecule within the CD cavity can be estimated by comparing the observed rotational strength from the ICD spectra with that calculated by the Kirkwood–Tinoco oscillator theory.[12] According to Harata and Uedaira, a positive ICD is observed when the electric dipole moment of the transition is parallel to the $C_7$ symmetry axis of the β-CD cavity.[7] Since the observed maximum at *ca.* 365 nm of the absorption spectrum of the guest **5** is due to the π→π* transition with an in-plane dipole moment which is roughly parallel to the long axis of the guest **5**, the magnitude of the ICD depends on the rigidity of the inclusion complex. Therefore, the larger molar ICD observed in the α-CD system

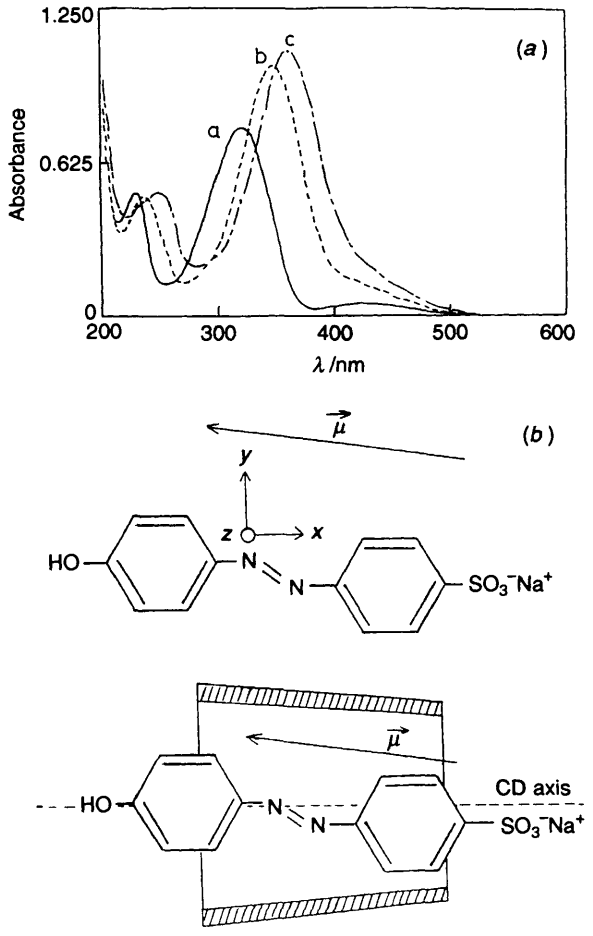


Fig. 2 (*a*) Electronic spectra of azobenzenes in 10% (v/v) ethanol–water; **a**, **b** and **c** represent *trans*-azobenzene **9**, 4-hydroxyazobenzene **10** and **5**, respectively; [azobenzene] = $4.84 \times 10^{-5}$ mol $dm^{-3}$. (*b*) Direction of the transition moment calculated for the absorption at the π–π* transition. Direction of the moment due to the π–π* transition is roughly parallel to the long axis of the CD cavity.

indicates a more intimate van der Waals contact between the interacting site of the guest and the inner wall of α-CD. The difference in the strength of these ICD spectra is reflected mainly in the stability of the inclusion complexes.[1] The ICD spectral patterns of the CD complexes of **5** are quite similar to each other, although the diameters of the cavity of α- (5.7 Å), β- (7.8 Å) and γ-CD (9.5 Å) are quite different. This fact indicates that the structure of these three inclusion complexes of **5** in water are very similar. The weaker effect of γ-CD upon **5** as compared with the effect of α-CD indicates the importance of a tight, size-compatible fit for chiral recognition by the CD molecule.

The shape and the sign of the ICD spectra of the β- and γ-CD inclusion complexes of the guest **8** are almost the same, which shows that the structures of these complexes are similar, but not the same as that of the α-CD complex [Fig. 1(*b*)]. Fig. 1(*b*) displays positive (*ca.* 350 nm) and negative (*ca.* 440 nm) split-type Cotton effects of β- and γ-CD complexes of **8**. The values of the opposite peaks of the ICD spectra are almost the same. The crossing points of the ICD couplet are practically coincident with the midpoint between the π→π* and n→π* transition bands. These split-type negative ICD signals may be characteristic of the dimerization of **8** within the chiral environment of a CD cavity.

*Assignment of the Electronic Absorption Band.*—In general, the azo dyes, such as **8**, were shown by linear dichroism studies to have only long-axis polarized transitions associated with their visible absorption bands. From Fig. 1, it is apparent that the spectrum of each guest molecule exhibits two or three main bands in the UV–VIS absorption spectral region. The UV band at *ca.* 250 nm can be attributed to the excitation of the π-electrons of the phenyl ring. The second one at 350–370 and 450 (shoulder) nm appearing in the visible region may be ascribed to the excitation band including the –N=N– group. It is apparent that the position and excitation of bands appearing in the UV–VIS region are dependent on the polarity of the medium and the electronic nature and position of the substituents on the phenyl rings.[13] However, the visible band is much influenced by the nature of the 4,4′-substituents as shown in Fig. 2(*a*). It is also characterized by a large red shift in alkaline solutions compared with acidic ones. This large red shift indicates that the π→π* transition of –N=N– group is influenced by an intramolecular charge transfer involving lone pairs on the $O^-$ group (Scheme 1).

**Table 1** Molecular orbital calculation of some azo molecules, $X-C_6H_4-N=N-C_6H_4-Y$

| Azo molecule | $M_x$[a] | $M_y$[a] | $M_z$[a] | $F$[b] | $E$[c]/nm |
|---|---|---|---|---|---|
| **9** | | | | | |
| X = H | 0.0 | 0.0 | 0.0 | 0.0 | 439 |
| Y = H | −5.78 | 1.50 | 0.0 | 0.565 | 296 |
| | −0.46 | −0.29 | 0.0 | 0.005 | 280 |
| | 0.002 | 0.001 | 0.0 | 0.000 | 280 |
| | −0.000 | −0.000 | 0.0 | 0.000 | 226 |
| **10** | | | | | |
| X = OH | 0.0 | 0.0 | 0.0 | 0.0 | 489 |
| Y = H | −5.94 | 1.47 | 0.0 | 0.581 | 303 |
| | −0.43 | 0.16 | 0.0 | 0.003 | 284 |
| | −0.22 | −0.24 | 0.0 | 0.002 | 280 |
| | 0.192 | −0.119 | 0.0 | 0.001 | 230 |
| **1** | | | | | |
| X = OH | −6.23 | 1.50 | −0.02 | 0.620 | 311 |
| $Y = SO_3^-$ | −0.03 | −0.85 | 0.001 | 0.012 | 288 |
| | −0.108 | 0.031 | 0.179 | 0.001 | 271 |
| | 0.792 | −2.43 | 0.005 | 0.124 | 248 |
| | −0.031 | 0.064 | 0.012 | 0.000 | 236 |

[a] $M_i$ = The transition moment in the direction of each axis in Fig. 2. [b] Oscillator strength. [c] Transition energy.

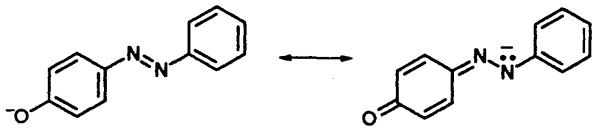

Scheme 1

When electron-donating substituents such as OH groups were introduced at the *para*-position with respect to the –N=N– group, the absorption maximum was shifted bathochromically.[13] This bathochromic shift is little changed by introducing an alkyl substituent but somewhat changed by an electron-withdrawing 4′-substituent such as a $SO_3^-$ group [Fig. 2(*a*)]. *trans*-Azobenzene **9** exhibits a well-separated n→π* and π→π* band. The longest weak absorption band (*ca.* 440 nm) is assigned to the n→π* band.[13] Little effect in the n→π* transition band was observed upon introducing electron-donating substituents such as an OH group. Therefore, the n→π* transition band became gradually overlapped with the tail of the π→π* band, particularly in the case of the 4-OH substituent [Fig. 2(*a*)].

The transition energies and moments of *trans*-azobenzene **9**, 4-hydroxyazobenzene **10**, and **1** are calculated by the CNDO/S method[14] and are given in Table 1. On the assumption that

compounds **9**, **10** and **1** are planar, the geometries were optimized by using the MINDO method.[15] Seventy singly-excited configurations were considered in the configuration interaction treatment. The experimental absorption maxima of **9**, **10** and **1** at 321, 350 and 358 nm are assigned to the theoretical $\pi\rightarrow\pi^*$ transition energy of 296, 303 and 311 nm, respectively. The direction of the transition moment ($\mu$) of the $\pi\rightarrow\pi^*$ absorption band almost coincides with the long axis of the azo molecule [Fig. 2(*b*)]. The angle $\theta$ between the molecular long axis and the transition moment ($\mu$) of **9**, **10** and **1** is only 15.0, 14.0 and 13.2° respectively. From the positive sign of the ICD signals observed in Fig. 1(*a*) at the $\pi\rightarrow\pi^*$ band, the direction of the moment ($\mu$) of the $\pi\rightarrow\pi^*$ transition of **5** turns out to be roughly parallel to the long axis of the CD cavity. On the other hand, the transition moment ($M_i$) and oscillator strength ($F$) of the $n\rightarrow\pi^*$ transition are almost zero as shown in Table 1. Since this forbidden transition has a $A''$ symmetry in the $C_s$ point group, the direction of the transition moment is perpendicular to the molecular plane. The value of $\theta$ between the $\mu$ of the $n\rightarrow\pi^*$ transition and the molecular long axis of **9** was obtained experimentally as 32° and 35° by measuring the dichroism spectra in the liquid and single-crystalline state.[16] A weak negative ICD signal around the $n\rightarrow\pi^*$ band was observed in the guest **5**–CD inclusion complexes [Fig. 1(*a*)]. This fact indicates that the $n\rightarrow\pi^*$ transition moment of the chromophore may not be parallel to the long axis of CD. Interestingly, the strength of the absorption band around the $n\rightarrow\pi^*$ region (450 nm) of **8** is appreciably larger than that of **5** (Fig. 3). This shoulder band almost disappeared upon addition of an organic solvent such as ethanol. Complexation with α-CD also decreases the strength of this shoulder band. These facts suggest that this band is related to the dimerization of **8**.† Fig. 3 shows the magnetic circular dichroism (MCD) spectra of **5** and **8** alone in aqueous solution. Ambiguous absorption bands which are strongly overlapped can be well separated in the MCD spectra.[17] In our case, a positive MCD band of **8** and a negative one of **5** originating mainly from the $n\rightarrow\pi^*$ transition are observed in the 400–500 nm region. Several MCD bands of **8** with opposite signs appear clearly in the short wavelength region (220–290 nm of line **b** in Fig. 3), although these bands are strongly overlapped in the absorption spectrum (line **b** in Fig. 3). The differences between these MCD spectra suggest that the solution structures of **5** and **8** are appreciably different.

*Molar Ratio of β-CD Complexes of* **5** *and* **8**.—Fig. 4(*a*) shows the differential absorption spectra in a large excess of β-CD. The change in absorbance of the $\pi\rightarrow\pi^*$ band (*ca.* 340 nm) is much larger than that of the $n\rightarrow\pi^*$ band (*ca.* 450 nm). Mole ratio plots of β-CD inclusion complexes of **5** and **8** are shown in Fig. 4(*b*) and (*c*) using the change in absorbance of these two bands. Mole ratio plots of **5** [Fig. 4(*b*) and (*c*)] and the Benesi–Hildebrand plot[2] at excess β-CD concentration clearly demonstrate the formation of a 1:1 inclusion complex. The absorbance of both bands decreases synchronously as the concentration of β-CD increases. The individual plot shows one

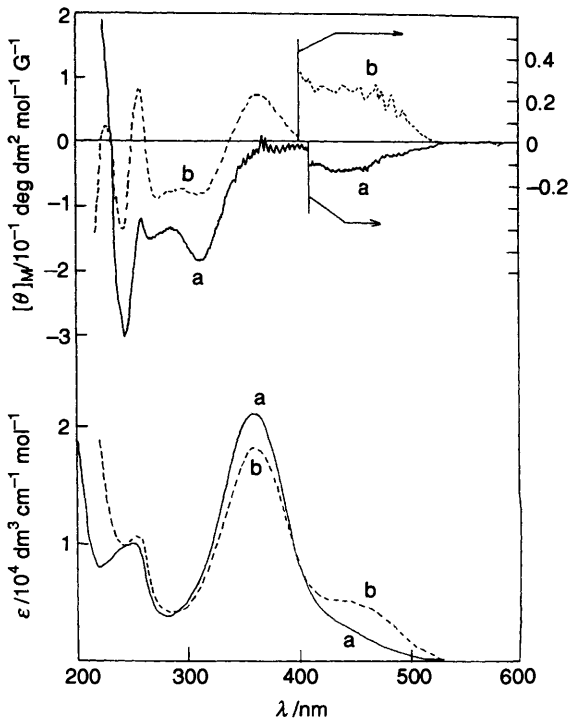


**Fig. 3** Magnetic circular dichroism (top) and absorption spectra (bottom) of **5** (**a**) and **8** (**b**) at pH 4 and 25 °C

inflection at about [β-CD]/[**5**] = 1. This is related to the fact that the **5**–βCD complex shows no split-type ICD spectrum. On the other hand, a complicated mole ratio plot ‡ is obtained in the **8**–βCD system [Fig. 4(*c*)], showing the formation of 2:1 (**8**:β-CD) and 2:2 complexes.§ As already shown in Fig. 1(*b*), the **8**–βCD complex shows a symmetrical negative split-type ICD spectrum. Both data strongly support the formation of a 2:2 (**8**:β-CD) inclusion complex and the interaction of two molecules of **8** in the form of a 1:1 (**8**:**8**) complex. As the β- and γ-CD complexes of **8** show similar ICD splittings [Fig. 1(*b*)], the structure of **8**–γCD should resemble that of **8**-βCD very closely in conformation and/or orientation within the CD cavity.

In general, a split ICD pattern may arise mainly from a dipole–dipole interaction between the electric transition moment of the two chromophores. The representative split-type ICD is the so-called exciton coupled-ICD. The magnitude of the Cotton effect is proportional to the magnitude of the transition moment of the chromophore, inversely proportional to the square of the distance between the two interacting chromophores, and depends on the angle between the two transition moments.[18,19] The 340 nm $\pi\rightarrow\pi^*$ intramolecular

† Measurement of the UV-VIS spectra of aqueous solutions of **8** at different concentrations allowed the characterization of the dimerization equilibrium:

$$28 \rightleftharpoons (\mathbf{8})_2 \qquad (K_d)$$

where $K_d = (1.5 \pm 0.1) \times 10^4$ mol$^{-1}$ dm$^3$. Addition of α-CD and ethanol to an aqueous solution of **8** would displace the dimerization equilibrium to the left. Solutions of **5** in water give rise to very little fluorescent emission. However, **8** shows a strong emission band at *ca.* 340 nm due to the dimer $(\mathbf{8})_2$ ($\lambda_{ex}$ = 250 nm).

‡ The data in Fig. 4(*c*) obtained by three independent experiments show strange breaks in the variation of $\Delta A$ with [β-CD]. This may be strongly related to the coupled-dimerization equilibrium of **8** with the inclusion equilibrium.

§ Fig. 4(*c*) shows two inflections at [β-CD]/[**8**] = 0.5 and 1. Strange to say, the absorption band at $n\rightarrow\pi^*$ and $\pi\rightarrow\pi^*$ does not always change synchronously. One explanation for the strange breaks is that 2:1 (**8**:β-CD) and 1:1 or 2:2 (**8**:β-CD) inclusion complexes are formed in water. Measurements of the UV-VIS and fluorescence spectra support the dimerization of **8**. Therefore, the breaks in Fig. 4(*c*) are best described by the equilibria:

$$28 \rightleftharpoons (\mathbf{8})_2$$

$$(\mathbf{8})_2 + \beta\text{-CD} \rightleftharpoons (\mathbf{8})_2\text{-}\beta\text{CD} \quad \text{(First break)}$$

$$(\mathbf{8})_2\text{-}\beta\text{CD} + \beta\text{-CD} \rightleftharpoons (\mathbf{8})_2\text{-}(\beta\text{CD})_2 \quad \text{(Second break point)}$$

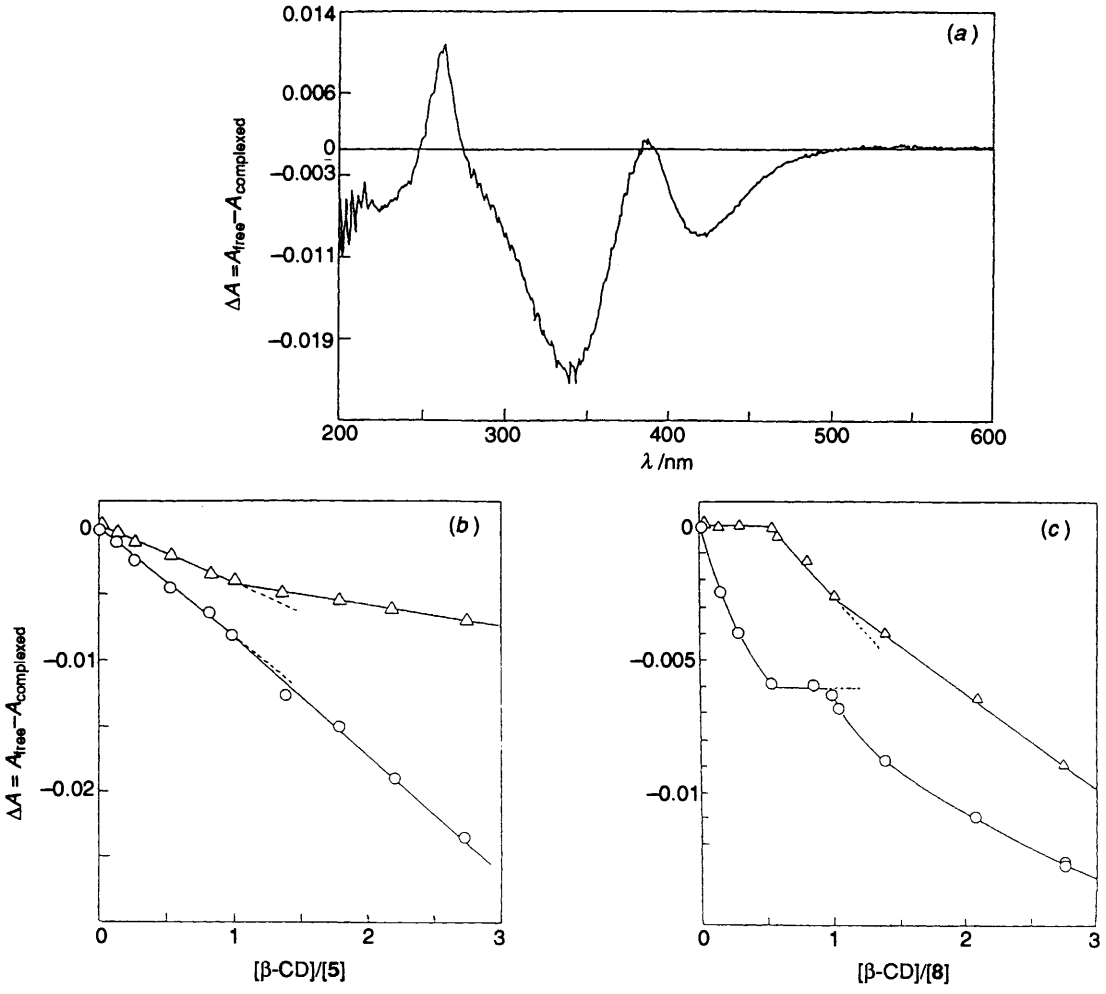


**Fig. 4** (*a*) Differential spectra of the β-cyclodextrin inclusion complex of **5**. [**5**] = 4.57 × $10^{-5}$ mol $dm^{-3}$ and [β-CD] = 1.26 × $10^{-4}$ mol $dm^{-3}$. (*b*) and (*c*) Mole ratio plots of β-cyclodextrin inclusion complexes of **5**(*b*) and **8**(*c*). [**5**] = [**8**] = 4.57 × $10^{-5}$ mol $dm^{-3}$.

charge-transfer transition of **8** is mainly directed along the long axis (*vide supra*). Judging from the model of the complexed molecules calculated by the exciton splitting and molecular orbital theory,[18] the negative split Cotton-effect observed both in the **8**–βCD and **8**–γCD inclusion complexes [Fig. 1(*b*)] should predict the angle between the associated chromophores in the complex.† In a structurally analogous azo dye such as Methyl Orange (MO), the MO–γCD 2:2 inclusion complex in which MO is considered to be in a parallel-plane head-to-tail arrangement has been found.[20] This head-to-tail arrangement would be adopted in the dimer to minimize repulsion between the negatively charged $SO_3^-$ groups. Clarke *et al.* reported that the environments around the MO chromophore in γ-CD and β-CD inclusion complexes are very different judging from the ICD spectral pattern.

*Structural Effect upon the ICD Spectral Pattern.*—Fig. 5(*a*) shows the ICD curves of the α-CD inclusion complexes with **1**, **5**, **7** and **8**. The ICD spectral pattern changes gradually depending upon the shape and size of the alkyl substituents of the guest molecules. The formation constants of the 1:1 α-CD inclusion complexes of **1**, **5**, **7** and **8** have been previously determined to be 6300, 4500, 1900 and 910 $dm^3$ $mol^{-1}$, respectively.[1] The maximum amplitude around the π–π* band (*ca.* 360 nm) of the ICD spectra depends roughly on the order in stability of their α-CDx inclusion complexes. The same spectral ICD pattern except for **8** would indicate that the structure of these α-CDx inclusion complexes is almost the same. As α-CDx is relatively rigid and the size of the cavity is strictly fixed, the penetration depth of the guest into the α-CDx cavity might be somewhat different, but the angle between the $C_6$ symmetry axis of α-CDx and the π–π* transition moment of the chromophore would be almost the same. Fig. 5(*b*) shows the ICD spectra of the β-CDx inclusion complexes. The spectra of the **1**–βCDx and **5**–βCDx complexes exhibit only positive signals around the π–π* transition and there is no spectral evidence of splitting due to dimer formation. This result is consistent with the formation of a single 1:1 complex and the structures of **1**–βCDx and **5**–βCDx resemble each other. Since the CD signal at the π–π* transition is positive, the transition moments of **1** and **5** are almost parallel to the $C_7$ symmetry axis of the β-CDx cavity. On the other hand, the positive and negative split-type ICD signals, which would be caused by dimerization of **8** within a chiral environment of the β-CDx cavity are observed as shown in Fig. 5(*b*). This unusual ICD spectrum pattern (negative and positive bands) is also observed in the **7**–γCDx and **8**–γCDx systems. The precise theoretical

† If the contribution of the exciton coupling is observed in the ICD spectrum, a split-type ICD spectrum having a zero intensity at $\lambda_{max}$ in the absorption spectrum should be observed. This is not the case for our ICD spectral data. The wavelength of the peaks in the ICD spectra of the **8**–CD complexes are in good agreement with those in the absorption spectra. However, some authors report that the crossover point of a split-type ICD spectrum does not always coincide with the absorption peaks. See refs. 3(*c*), 3(*d*), 11(*c*) and 20.

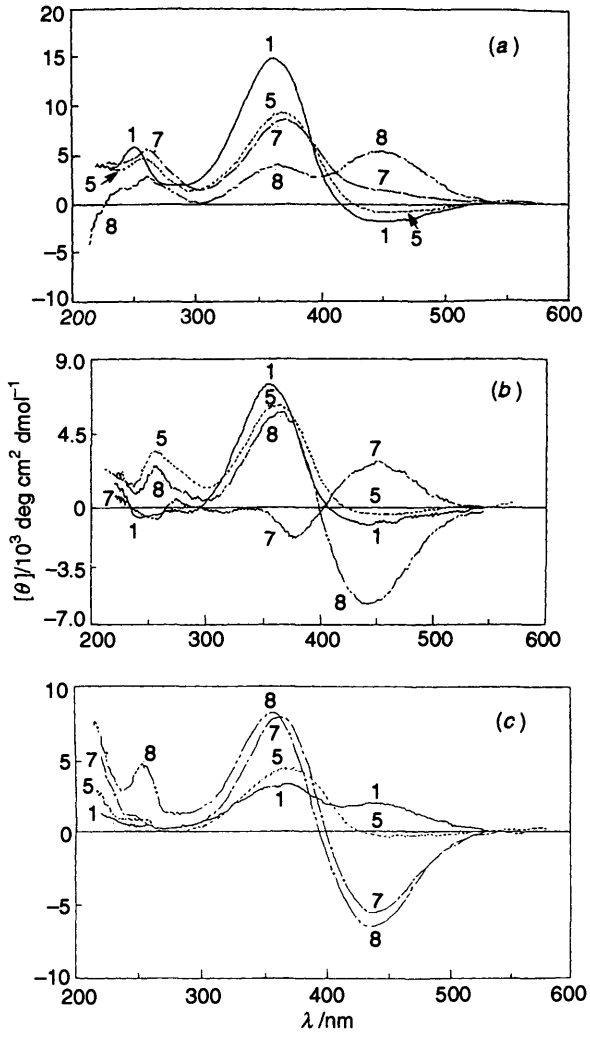


Fig. 5 ICD spectral pattern of the α-cyclodextrin (*a*), β-cyclodextrin (*b*) and γ-cyclodextrin (*c*) inclusion complexes with $HA^-$ species of **1**, **5**, **7** and **8** (at pH 4)

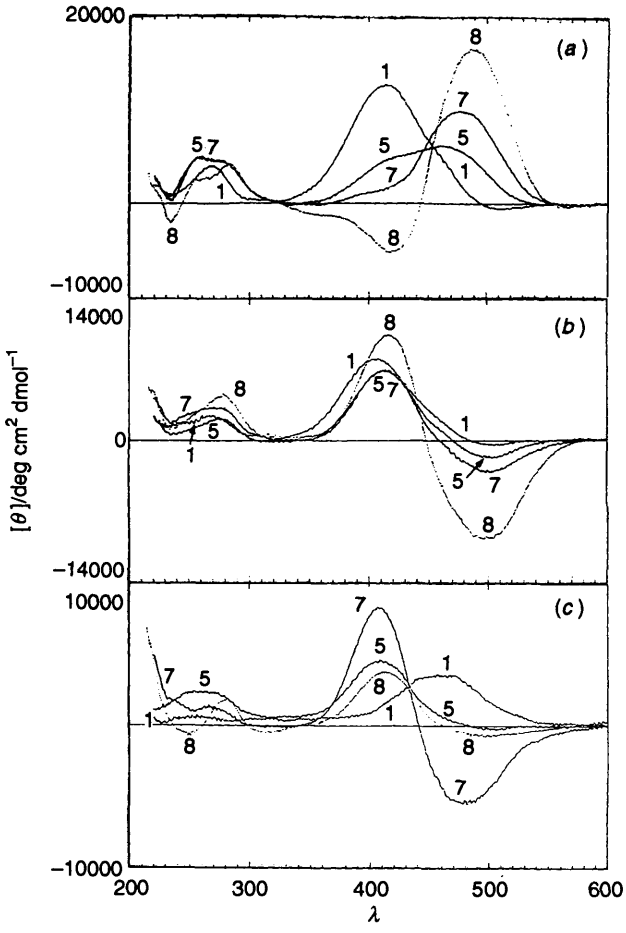


Fig. 6 ICD spectral pattern of the α-cyclodextrin (*a*), β-cyclodextrin (*b*) and γ-cyclodextrin (*c*) inclusion complexes with $A^{2-}$ species of **1**, **5**, **7** and **8** (at pH 12)

treatment of these unusual ICD spectrum patterns is now in progress.*

The various ICD spectra of **1**–, **5**–, **7**– and **8**–γCDx are shown in Fig. 5(*c*). In general, the weaker effect of γ-CDx upon the strength of the ICD spectrum of **1**– and **5**–γCDx is due to the lack of a tight and size-compatible fit for recognition as compared with the effect of α-CDx and β-CDx. However, the relatively strong splitting ICD pattern in **7**–γCDx and **8**–γCDx systems would be ascribed to dimerization of the chromophore. The structure of **7**–γCD resembles that of **8**–γCD and **8**–βCD. Judging from the ICD spectrum patterns, the structures of **1**–γCD and **5**–γCD are considerably different from those of **7**–γCD and **8**–γCD. Subtle changes in the size and shape of the alkyl substituent of the phenol moiety of the guests **1**–**8** have a crucial influence upon the ICD spectral pattern of the CD complexes. Furthermore, in all the systems, a positive enhancement located within the 300–400 nm region is clearly observed except for **7**–βCD. This fact suggests that the guest long-axis transition with respect to the molecular axis of the CD is almost parallel, although the orientation, tightness and depth of the guest molecule in the CD cavity are appreciably different.

*Ionization Effect upon the ICD Spectral Pattern.*—Aqueous solutions of **1**–**8** exhibit a red–orange colour change with increasing pH of the solution. This occurs in the pH range 7.88–8.70 ($pK_a$) due to the acid-dissociation equilibrium shown in eqn. (3).[2] The $\lambda_{max}$ values of the acid ($HA^-$) forms of **1**–**8** are

$$HA^- \rightleftharpoons A^{2-} + H^+ \quad (3)$$

almost the same, however those of the base ($A^{2-}$) forms tend to shift drastically to longer wavelengths. The wavelengths of the $A^{2-}$ forms of **1**, **5**, **7** and **8** are 442 (420sh), 460, 469 and 477 nm, respectively. This red shift is caused by the keto–enol tautomeric equilibrium shown in Scheme 1. Introducing an alkyl substituent to the *ortho*-position at the 4-$O^-$ group of **1**–**8** would enhance the formation of the keto species. Therefore, since the inclusion reaction is coupled to the keto–enol equilibrium, the interpretation of the ICD spectral pattern of $A^{2-}$–CD is more difficult than that of $HA^-$–CD.

Fig. 6(*a*) shows the ICD pattern of the $A^{2-}$–αCD inclusion complexes with **1**, **5**, **7** and **8**. A gradual change is observed in the **1**($A^{2-}$)–, **5**($A^{2-}$)– and **7**($A^{2-}$)–αCD systems. Since the guest long-axis transition moment would be almost parallel to the molecular axis of the CD, this gradual change seems to be related to the tautomeric equilibrium and/or the depth of incorporation. The ICD spectrum of **8**($A^{2-}$)–αCD is quite different from that of **1**($A^{2-}$)–, **5**($A^{2-}$)– and **7**($A^{2-}$)–αCD. The

* It is possible that the superposition of two independent CD bands having opposite signs leads to the observation of an apparent split-type ICD pattern. However, the split-type ICD patterns in our case are only observed in the β- and γ-CD complexes of a hydrophobic guest such as **8**. Guests **7** and **8** tend to aggregate in water as compared with the guests **1** and **5**. Furthermore, β- and γ-CD have a larger cavity which could encapsulate the dimer of the guest molecule.

structures of $1(A^{2-})$–, $5(A^{2-})$– and $7(A^{2-})$–βCD are quite similar to each other as judged by the ICD pattern shown in Fig. 6(*b*). The splitting pattern observed in $8(A^{2-})$–βCD would be caused by the dimerization of $8(A^{2-})$. This is also the case for the $7(A^{2-})$–γCD system. The ICD pattern in Fig. 6(*c*) indicates that $5(A^{2-})$–γCD and $8(A^{2-})$–γCD have similar structures. Interestingly, it can be seen from Fig. 6(*a*), (*b*) and (*c*) that the structures of the α- and β-CD inclusion complexes of $1(A^{2-})$ are quite different from that of $1(A^{2-})$–γCD. Finally, it is noteworthy that the alkyl substituents of **1**–**8** play an important role in causing the sign and amplitude of the Cotton effect, resulting in the various ICD spectral patterns.

## References


1 N. Yoshida, A. Seiyama and M. Fujimoto, *J. Phys. Chem.*, 1990, **94**, 4246; N. Yoshida and K. Hayashi, *J. Chem. Soc., Perkin Trans. 2*, 1994, 1285.

2 N. Yoshida, A. Seiyama and M. Fujimoto, *J. Phys. Chem.*, 1990, **94**, 4254.

3 (*a*) H. Yamaguchi and S. Abe, *J. Phys. Chem.*, 1981, **85**, 1640; (*b*) H. Shimizu, A. Kaito and M. Hatano, *Bull. Chem. Soc. Jpn.*, 1981, **54**, 513; *J. Am. Chem. Soc.*, 1982, **104**, 7059; (*c*) R. J. Clarke, J. H. Coates and S. F. Lincoln, *J. Chem. Soc., Faraday Trans. 1*, 1984, **80**, 3119; (*d*) R. J. Clarke, J. H. Coates and S. F. Lincoln, *J. Chem. Soc., Faraday Trans. 1*, 1986, **82**, 2333; (*e*) H. Yamaguchi and M. Higashi, *J. Inclusion Phenom.*, 1987, **5**, 725; (*f*) H. Yamaguchi, M. Higashi, J. Nakayama and M. Hoshino, *J. Inclusion Phenom., Mol. Recognit. Chem.*, 1990, **9**, 253; (*g*) K. Kano, K. Yoshiyasu, H. Yasuoka, S. Hata and S. Hashimoto, *J. Chem. Soc., Perkin Trans. 2*, 1992, 1265; (*h*) S. Li and W. Purdy, *Anal. Chem.*, 1992, **64**, 1405; (*i*) J. M. Schuette, T. T. Ndou and I. M. Warner, *J. Phys. Chem.*, 1992, **96**, 5309; (*j*) M. Kamiya, S. Mitsuhashi, M. Makino and H. Yoshioka, *J. Phys. Chem.*, 1992, **96**, 95.

4 B. B. Myhr and J. G. Foss, *Biopolymers*, 1966, **4**, 949; M. Hatano, M. Yoneyama, Y. Sato and Y. Kawamura, *Biopolymers*, 1973, **12**, 2423.

5 J. H. Perrin and D. A. Nelson, *J. Pharm. Sci.*, 1973, **25**, 125; E. Daniel and J. T. Yang, *Biochemistry*, 1973, **12**, 508; J. H. Perrin, *J. Pharm. Sci.*, 1973, **25**, 208.

6 A. Blake and A. R. Peacocke, *Biopolymers*, 1967, **5**, 383; C. Formoso, *Biochem. Biophys. Res. Commun.*, 1973, **50**, 999; C. Formoso, *Biopolymers*, 1974, **13**, 909; P. E. Schipper and B. Norden, *Chem. Phys. Lett.*, 1980, **70**, 17; K. Kano, K. Yoshiyasu and S. Hashimoto, *Chem. Lett.*, 1990, 21.

7 K. Harata and H. Uedaira, *Bull. Chem. Soc. Jpn.*, 1975, **48**, 375.

8 P. E. Schipper and A. Rodger, *J. Am. Chem. Soc.*, 1983, **105**, 4541; M. Kodaka, *J. Phys. Chem.*, 1991, **95**, 2110.

9 T. Hoshino, V. Matsumoto, N. Harada and T. Goto, *Tetrahedron Lett.*, 1981, **22**, 3621; T. Goto and T. Kondo, *Angew. Chem., Int. Ed. Engl.*, 1991, **30**, 17.

10 V. Buß, *Angew. Chem.*, 1991, **30**, 869; V. Buß and C. Reichardt, *J. Chem. Soc., Chem. Commun.*, 1992, 1636; N. Berova, D. Gargiulo, F. Derguini, K. Nakanishi and N. Harada, *J. Am. Chem. Soc.*, 1993, **115**, 4769.

11 (*a*) M. Hatano, M. Yoneyama, Y. Sato and Y. Kawamura, *Biopolymers*, 1973, **12**, 2423; (*b*) H. Yamaguchi, *J. Incl. Phenom.*, 1984, **2**, 747; (*c*) M. Suzuki, M. Kajtar, J. Szejtli, M. Vikmon and E. Fenyvesi, *Carbohydr. Res.*, 1992, **223**, 71.

12 J. P. Kirkwood, *J. Chem. Phys.*, 1937, **5**, 479; I. Tinoco, Jr., *Adv. Chem. Phys.*, 1962, **4**, 113.

13 H. H. Jaffé, Si-J. Yeh and R. W. Gardner, *J. Mol. Spectrosc.*, 1958, **2**, 120; M. Robin and W. T. Simpson, *J. Chem. Phys.*, 1962, **36**, 580; J. Kroner and H. Bock, *Chem. Ber.*, 1968, **101**, 1922; B. Uno, Y. Matsuhisa, K. Kano and T. Kubota, *Chem. Pharm. Bull.*, 1984, **32**, 1691; C. L. Forber, E. C. Kelusky, N. J. Bunce and M. C. Zerner, *J. Am. Chem. Soc.*, 1985, **107**, 5884.

14 H. Bauman, CNDUV (*QCPE* No. 333), 1977.

15 M. J. S. Dewar and W. Thiel, *J. Am. Chem. Soc.*, 1977, **99**, 4899.

16 K. Toda, S. Nagaura, M. Watanabe, M. Kamae and K. Honda, *Nippon Kagaku Kaishi*, 1975, 459; M. B. Robin and W. T. Simpson, *J. Chem. Phys.*, 1962, **36**, 580.

17 Y. K. Mo, R. E. Linder, G. Barth, E. Bunnenberg and C. Djerassi, *J. Am. Chem. Soc.*, 1974, **96**, 3311; N. Igarashi, A. Tajiri and M. Hatano, *Bull. Chem. Soc. Jpn.*, 1981, **54**, 1511; M. Higashi, H. Yamaguchi, T. Machiguchi, T. Hasegawa and H. Baumann, *Helv. Chim. Acta*, 1992, **75**, 1880.

18 N. Harada and K. Nakanishi, *Acc. Chem. Res.*, 1972, **5**, 257.

19 N. Harada and K. Nakanishi, *Circular Dichroic Spectroscopy—Exciton Coupling in Organic Stereochemistry*, University Science Books, Mill Valley, CA, 1983.

20 R. J. Clarke, J. H. Coates and S. F. Lincoln, *Carbohyd. Res.*, 1984, **127**, 181.


*Paper* 4/04034A
*Received* 4*th July* 1994
*Accepted* 15*th August* 1994